



LOW-CYCLE FATIGUE LIMIT ON SEISMIC ROTATION CAPACITY FOR US STEEL MOMENT CONNECTIONS

Kyungkoo LEE¹ and Bozidar STOJADINOVIC²

SUMMARY

A cyclic yield-line plastic hinge model is developed to estimate the rotation capacity of fully-restrained steel moment connections designed for moment-frame structures in the US under seismic load conditions. The geometry of the beam after local buckling occurs in the plastic hinge is modeled using the yield-line approach. A simplified force-displacement relation for the plastic hinge is proposed based on large deformations and plastic moment at the yield lines using the principle of virtual work.

Two limit states are considered using the cyclic yield-line plastic hinge model. First, post-peak connection strength degradation due to local and lateral-torsional buckling is used to establish a connection rotation limit similar to the limit used in FEMA-350. Second, low-cycle fatigue crack initiation model based on a cumulative local strain concept at the critical yield line is used to predict crack initiation at the creases of the local buckles in the plastic hinge and, thus, limit plastic hinge rotation. A comparison of connection rotation capacities recorded in recent SAC Joint Venture tests is presented to validate the proposed cyclic yield-line plastic hinge model.

The proposed cyclic yield-line plastic hinge model is a calibrated analytical model for estimating connection rotation capacity. This model is intended for use by designers to develop new connections before the required proof-tests.

INTRODUCTION

Steel moment connections in the US after the 1994 Northridge earthquake have been investigated because of their unexpectedly poor performance. These investigations (FEMA-350 [1]) produce design recommendations for new steel frame structures. At the core of these design recommendations is requirement that fully-restrained moment connections have total rotation capacity exceeding 4% radian without losing more than 20% of their maximum resistance. To demonstrate this, a pre-qualification test requirement was imposed. Each new connection type is required to pass a series pre-qualification test

¹ Doctoral Candidate, 721 Davis Hall #1710, Department of Civil and Environmental Engineering, University of California, Berkeley, CA 94720-1710, USA, kklee@ce.berkeley.edu.

² Associate Professor, 721 Davis Hall #1710, Department of Civil and Environmental Engineering, University of California, Berkeley, CA 94720-1710, USA, boza@ce.berkeley.edu.

conducted using a prescribed procedure. Such pre-qualification test approach was adopted by SAC and codified in FEMA-350 and AISC documents because rotation capacity of steel moment connections could not be reliably predicted using conventional analytical models, such as finite element or fracture mechanics models. Even though this approach is safe, it is expensive, and it hampers development of new connection designs.

Failure of pre-qualified steel moment connections after only a few cycles of high-amplitude deformation was observed in pre-qualification tests. Such ductile failure occurred after significant buckling of the beam in the plastic hinge region. It manifested itself through gradual propagation of cracks in the creases of the beam buckled shape. Such low-cycle fatigue failure occurs primarily because significant amounts of plastic deformation are accumulated during each cycle. While low-cycle fatigue resistance is not an explicit requirement of the connection pre-qualification test procedure, resistance to this failure mode is important for seismic structural design because steel structures may have to endure a number of significant earthquakes, each having a few cycles of large deformation demand, which may pose a cumulative connection fracture risk.

In this paper, a simple yield-line plastic hinge model is proposed to model local buckling of a beam in a moment connection in order to estimate the seismic rotation capacity of typical US steel moment connections. This approximate method, which uses a plastic collapse mechanism approach, is based on interpretation of experimental evidence on the shape of the buckled plastic hinge region. Both ultimate strength degradation and low-cycle fatigue caused by plastic strain accumulation at critical points in the plastic hinge region are considered. This method fills the gap between finite element numerical models and pre-qualification testing and improves our ability to design new steel moment connection capable of passing the current pre-qualification requirements.

LITERATURE REVIEW

Local buckling

Local buckling is expected to occur in the plastic hinge region of the beam in pre-qualified WUF-W, Reduced Beam Section (RBS), Free Flange and Cover Plate moment connections prescribed in the FEMA-350 design guidelines. Several different methods exist to investigate local buckling:

- Empirical methods: these methods are based on statistical analysis of test data. They have the realism of data, but they also suffer from the large scatter of test result.
- Classical theoretical methods: these methods are based on integrating the moment-curvature relationship for a plastic hinge and can be used to determine the rotation capacity corresponding to maximum moment without buckling. They are conservative, given that local buckling causes strength degradation which they can not capture.
- Finite element methods: these numerical methods can be used to model local buckling and the resulting strength degradation, but are time consuming and complex.
- Approximate method: these methods are based on modeling the empirically observed plastic collapse mechanisms formed by local buckling. They may offer a desirable mix of accuracy and easy of use for practical design.

Gioncu and Petcu [2], Anastasiadis, Gioncu and Mazzolani [3] and Möller [4] introduced the yield-line concept to model the buckled shapes observed in experiments. They constructed yield-line models and used this plastic mechanism to determine rotation capacity of European H-section beams. They showed that the yield-line model produces strength degradation rates and rotation capacities in good agreement with both monotonic and cyclic test results.

Low-cycle fatigue

Low-cycle fatigue limit state, observed during pre-qualification tests of moment connections as ductile tearing of the metal in the creases of the beam plastic hinges after a few large-amplitude cycles, is indirectly accounted for in the pre-qualification test requirements. On the other hand, low-cycle fatigue resistance has been extensively studied in bridge structures [5]. Manson-Coffin's rule is usually used to interpret the data obtained from component constant- and variable-amplitude cyclic tests. Ballio and Castiglioni [6], Bernuzzi, Calado and Castiglioni [7] suggested a low-cycle fatigue approach for design of steel structural connections. They used the linear damage accumulation Miner's rule together with the rain flow cycle counting method to assess damage under variable-amplitude loading.

It has been observed that plastic behavior of steel under cyclic loading is nonlinear and history dependent. Furthermore, the stress-strain response of steel changes significantly with cyclic straining into the plastic range. Thus, fatigue life in the plastic range may be more accurately described as a function of the cyclic strain amplitude than the cyclic stress amplitude. Low-cycle fatigue test data for a family of different constant strain amplitude tests are usually displayed using a logarithmic plot of strain amplitude versus the number of cycles to failure at that amplitude. Either plastic strain amplitude or total strain amplitude may be used. These plots will typically show an approximately linear relation between the number of cycles to failure and strain amplitude in the log-log space (Fig. 1). Using a log-log linear approximation, expected fatigue life may be computed from an $S-N$ curve suggested by Manson and Coffin as follows:

$$NS^m = K \quad (1)$$

where N is the number of cycles to failure, S is a constant total or plastic strain amplitude, and K and m are material properties obtained from tests. Experiments show that m has a value of approximately 2 for plastic strain amplitudes and approximately 3 for total strain amplitudes.

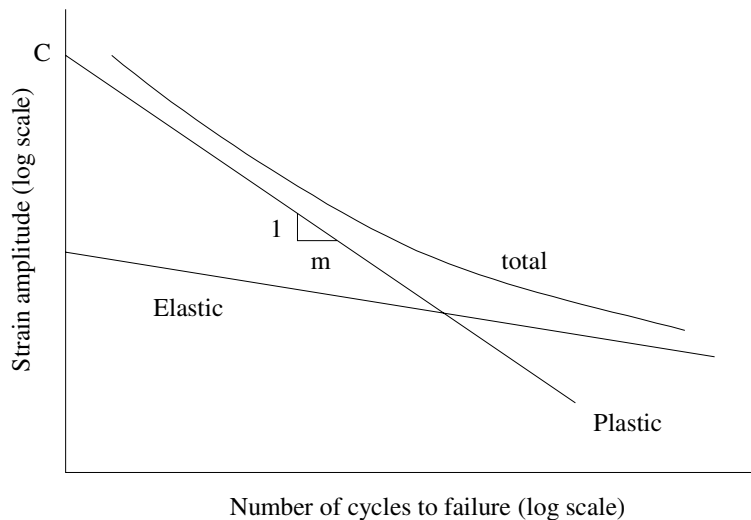


Fig. 1. S-N curve: Strain amplitude versus number of cycles to failure [8].

Variable amplitude loading, which occurs during earthquakes, produces strain cycles of variable amplitude. A cycle counting method, such as the rain-flow method, may be used to count the number of cycles in each strain range. The number of cycles to failure may, then, be determined using the Manson-Coffin relation that gives the numbers of cycles to failure under constant strain range. Adopting Miner's rule that accumulates damage induced by cycles of constant strain amplitude linearly, a damage index D , can be expressed as follows:

$$D = \sum_{i=1}^j \frac{n_i}{N_i} \quad \text{and} \quad n_{tot} = \sum_{i=1}^j n_i \quad (2)$$

where n_i is the number of cycles at any given amplitude level S_i , N_i is the number of cycles to failure under a constant amplitude S_i , and n_{tot} is total number of variable amplitude strain cycles. More generally, equivalent amplitude and number of strain cycles can be computed using a damage index, total number of cycles and magnitudes of variable amplitudes by substituting the definition of equivalent number of cycles and Miner's rule into Manson-Coffin relation [7]:

$$D = \frac{n_{tot}}{N_{eq}} \rightarrow N_{eq} = \frac{n_{tot}}{D} \quad (3)$$

$$N_{eq} S_{eq}^m = K \rightarrow S_{eq}^m = \sum_{i=1}^{n_{tot}} \frac{n_i S_i^m}{n_{tot}}$$

METHODOLOGY: YIELD-LINE PLASTIC HINGE MODEL

Local buckling of the flange and/or the web of compact steel W-shapes occurs after substantial yielding. In steel moment frames, such yielding is assumed to occur only in the plastic hinge region of the beams. Note, however, that the method presented herein is quite general and may be applied to other local buckling problems. Deformation capacity of the beam plastic hinge will, therefore, depend on the rotation enabled by the local buckling mechanism that takes shape after buckling.

Fig. 2 shows a flow chart for implementing the yield-line plastic hinge (YLPH) model for both monotonic and cyclic loading. A cross-section is "fiberized" (discretized into uni-axial fibers) first. Then, the expected buckled shape is defined. Under monotonic loading, only one buckled shape shown in Fig. 3 corresponding to the flange in compression is used. This shape is derived based on experimental evidence. Under cyclic loading, a composite buckled shape comprising two buckled shapes shown in Fig. 4, one for the top and the other for the bottom flange is used. In either case, the buckled shape is treated as an initial imperfection. Using the buckled shape geometry, the kinematics of the yield-line mechanism is derived to relate beam plastic hinge rotation increments to increments of yield-line rotation and flange and web axial shortening in the entire cross section of the plastic hinge. Assuming a fully plastic stress state at yield-lines, a relation between external and internal forces acting on the yield-line plastic hinge fibers is derived using the principle of virtual work. The principle of virtual work (a weak form of equilibrium of the yield-line moments and axial forces in the plastic hinge) is formulated to compute the effective stress distributions in the buckled region. In the part of the cross-section where buckling is not expected to occur, and the cross-section plane is expected to remain plane an elastic-perfectly-plastic constitutive relation for fibers is used to establish an elastic-perfectly-plastic stress distribution in the cross section. The complete stress distribution can be integrated across the entire cross-section area. The cross-section model is iterated on the buckled flange displacement until equilibrium between internal and external forces is achieved. Finally, the available rotation capacity can be computed using force or deformation limit state criteria. The strength limit state defines critical strength degradation, either below the nominal plastic strength or below 80% of the maximum strength. The deformation limit state defines fracture initiation in a flange when ultimate tensile strain is attained at a critical point of a critical yield-line in the buckled region. These steps in implementing the yield-line plastic hinge model are further explained in the following sections of this paper.

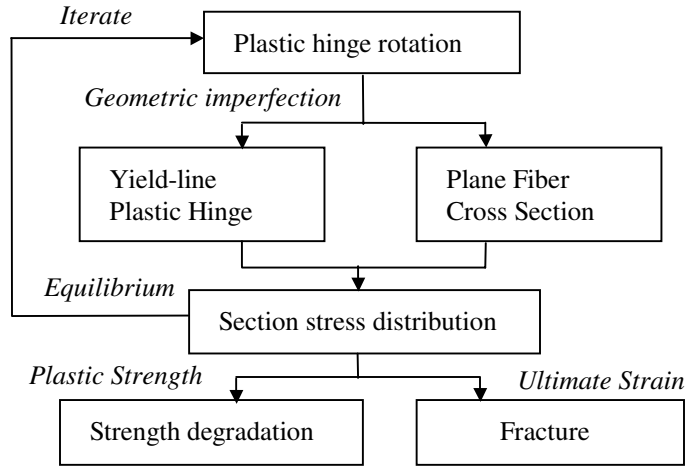


Fig. 2. Flow-chart for the YLPH model under monotonic loading.

Local buckling initiation

The length of the beam plastic region is set as the flange buckling wavelength, as shown in Fig. 3. To compute the flange buckling wave length, Lay's equation for plate buckling wave length was used. Assuming the flange fully yields before inelastic local buckling and considering rotational restraint provided the web against flange local buckling Lay [9] computed the half wavelength of the flange buckle, L_f , corresponding to the minimum critical buckling stress as follows:

$$2L_f = \beta b_f \approx 0.6 \left(\frac{t_f}{t_w} \right)^{\frac{3}{4}} \left(\frac{h}{b_f/2} \right)^{\frac{1}{4}} b_f \quad (4)$$

where b_f is flange width, t_f is flange thickness, t_w is web thickness, d_b is beam depth, and $h=d_b-2t_f$, respectively. For a beam under moment gradient, a full wavelength of the beam flange local buckle was taken as the length the plastic hinge region.

A beam plastic hinge cross section just prior to local buckling of the compression flange can be expected to develop stress values larger than the yield stress in the flange and in a portion of the web. Thus, computing the nominal moment resistance of the beam cross section underestimates the resistance of the beam in the connection. To compute the moment resistance of a plastic hinge, an expression for the probable peak plastic hinge moment at a plastic hinge (FEMA 350 Ch 3 equation (3-1) [1]) was used:

$$M_{pr} = C_{pr} R_y Z_e F_y \quad (5)$$

where M_{pr} is probable peak plastic hinge moment, C_{pr} is a factor to account for the peak connection strength using equation (3-1) in FEMA-350, R_y is a coefficient to account for yield stress over-strength obtained from the AISC Seismic Provisions, Z_e is the effective plastic modulus of the section at the location of the plastic hinge, and F_y is the specified minimum yield stress of the material of the yielding element. This expression was used to compute the critical stress (a modified yield stress) for the elastic-perfectly plastic constitutive relation of the plastic hinge forming at the yield-lines.

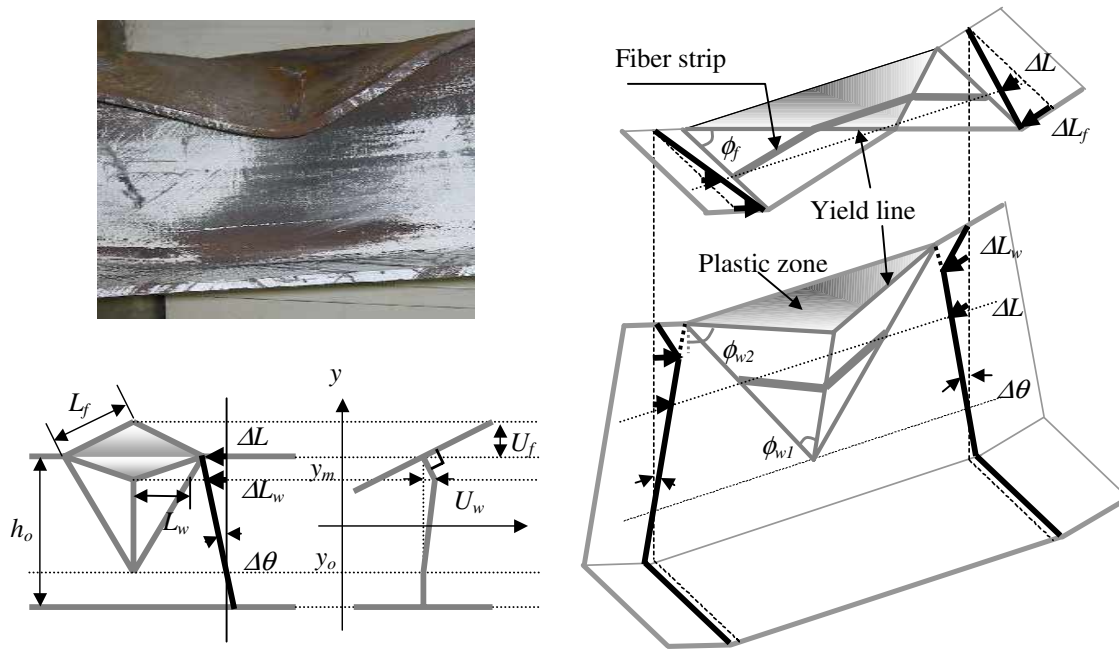


Fig. 3. Monotonic YLPH model deformation.

Geometry and kinematics

Geometry of the yield-line plastic hinge model is shown in Fig. 3. Geometric assumptions and constraints are as follows: 1) Flange and web buckling wavelengths, L_f and L_w , remain unchanged during plastic rotation; 2) The center of rotation point of the plastic hinge mechanism, defined by y_o , does not move while rotation increases; 3) The flange remains perpendicular to the web during plastic hinge rotation; 4) The unbuckled boundary sections remain plane at either side of the plastic hinge; and 5) Boundary condition at the joint between the flange and the web is a simple support.

Let ΔL be a yield-line mechanism displacement with respect to the un-deformed state and $\Delta\theta$ be a yield-line mechanism rotation corresponding to beam plastic hinge rotation, as shown in Fig. 3. From geometry, the following stands:

$$\Delta\theta = \frac{\Delta L_f}{h_o/2 - y_o} = \frac{\Delta L_w}{y_m - y_o} \quad (6)$$

where ΔL_f is a flange displacement, ΔL_w a displacement at location y_m where maximum web buckling amplitude occurs, while y_o defines the location of the center of rotation of the plastic hinge mechanism.

Flange buckling wavelength L_f can be computed using Equation (4). Then, web buckling wavelength can be computed from geometry using similar triangles. Under the assumption that flange and web buckling wavelengths, L_f and L_w , are unchanged, and using Pythagoras' Theorem, each flange and web buckling amplitude can be expressed in terms of its yield-line mechanism displacement as:

$$\begin{aligned} U_f^2 &= L_f^2 - [L_f - \Delta L_f]^2 \\ U_w^2 &= L_w^2 - [L_w - \Delta L_w]^2 \end{aligned} \quad (7)$$

Assuming that the flange and the web twist to keep the flange perpendicular to web, the following relation between flange buckling amplitude and web buckling amplitude holds:

$$\frac{U_f}{b_f/2} = \frac{U_w}{h_o/2 - y_m} \quad (8)$$

Location where maximum web buckling amplitude occurs, defined by y_m , is obtained by inserting Equations (6) and (7) into Equation (8) regardless of the magnitude of plastic hinge rotation increment $\Delta\theta$. This completes the kinematics of the YLPH model: all deformation quantities in the model can now be computed given a value of the beam plastic hinge rotation.

Flange and web yield-line mechanisms within a plastic hinge include plastic zone, where axial shortening occurs, and yield lines where plastic rotation occurs. Assume that beam cross-section deformations before buckling are small enough to be neglected, except for axial deformation along the beam axis. Axial deformations of the flange and the web yield-line mechanisms after buckling are shown in Fig. 3. Consider an axial deformation of a fiber strip in yield-line mechanisms. Such axial deformation may be decomposed into shortening in the plastic zone and rigid body motion caused by yield-line rotations. With the assumption that flange and web buckling wavelengths are unchanged, the increment of flange and web buckling amplitude can be related to the increment of axial displacement ΔL and yield-line rotations $\Delta\theta_i^{YL}$ as follows:

$$\begin{bmatrix} \Delta\theta_1^{YL} \\ \Delta\theta_2^{YL} \end{bmatrix} = [A] \cdot \frac{\Delta L}{U} \quad (9)$$

$$[A] = \begin{bmatrix} 1 \\ 1/\cos\phi_f \end{bmatrix} \text{ for a flange fiber}$$

$$= \begin{bmatrix} 1/\cos\phi_{w1} \\ 1/\cos\phi_{w2} \end{bmatrix} \text{ for an upper web fiber}$$

$$= \begin{bmatrix} 1/\cos\phi_{w1} \\ 1 \end{bmatrix} \text{ for a lower web fiber}$$

where U is the buckling amplitude of a fiber and ϕ_f , ϕ_{w1} , and ϕ_{w2} are the angles of the inclined yield lines with respect to the cross section on which axial deformation is being applied, as shown in Fig. 3.

Under cyclic loading, two buckling shapes must be considered. If the flange that buckled in compression straightens completely, such that there is no residual buckling shape, when it goes into tension, as shown in Fig. 3, a relation between a yield-line mechanism displacement ΔL and rotation $\Delta\theta$ under loading and reverse loading can be obtained using equation (6) as if the loading was monotonic. If, on the other hand, the flange that buckled does not straighten completely when in tension, a residual buckled shape, shown in Fig. 4, must be considered. In this case, the relation between ΔL and $\Delta\theta$ can be obtained by a superposition of two opposite monotonic buckling shapes, one for each side of the beam, as:

$$\Delta L = \Delta L^i + \Delta L^b \quad (10)$$

$$\Delta\theta = \Delta\theta^i + \Delta\theta^b$$

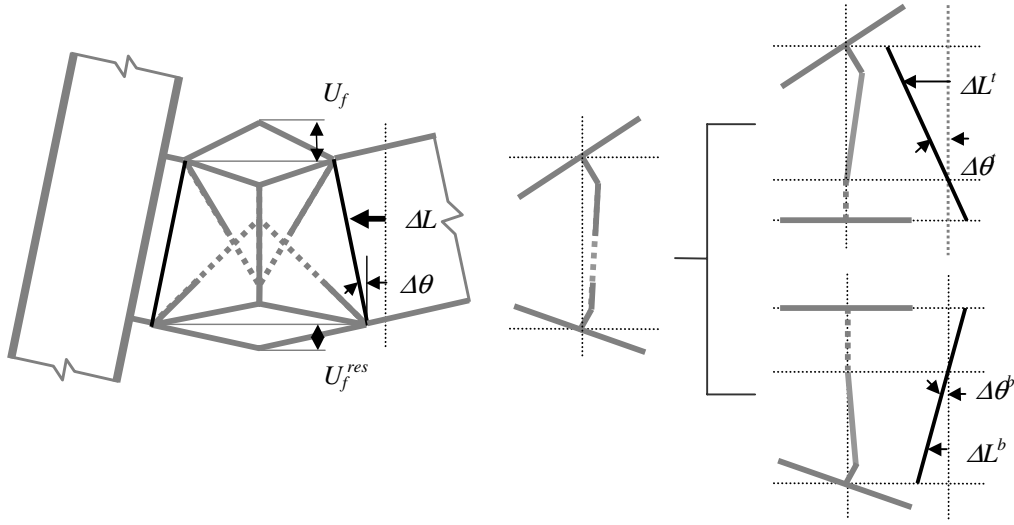


Fig. 4. Cyclic YLPH model with a residual buckling shape.

Principle of virtual work

Consider a fiber strip with unit width and a yield-line mechanism shown in Fig. 5. Assuming an elastic-perfectly plastic moment-curvature relation for a yield line cross-section, the plastic bending moment per unit length of the yield line is $m_p = f_y t^2 / 4$. This plastic moment is assumed to act on the entire length of all yield lines in this yield-line mechanism. The axial force working on the axial shortening of the fiber strip works externally. Internal work is assumed to be done by the bending moments working on yield-line rotations and by the axial force working on axial shortening of the plastic zones between the yield lines. Since axial deformation is composed of shortening and rigid body rotation, the principle of virtual work can be expressed as:

$$N \cdot \Delta L = \sum_{i=1}^2 m_p \cdot \Delta \theta_i^{YL} \quad (11)$$

where N is an externally applied axial force over unit width of the fiber strip. Then, the axial force is obtained by inserting Equation (9) into Equation (11) as follows:

$$N = \frac{m_p}{U} \cdot [A_1 + A_2] \quad (12)$$

where A_1 and A_2 are components of matrix $[A]$ in equation (9).

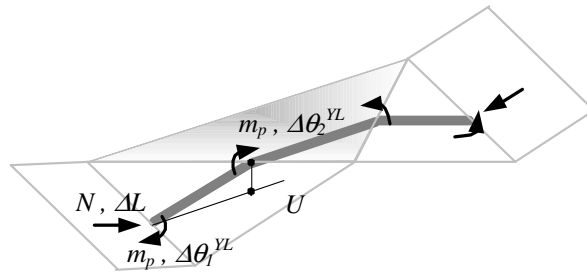


Fig. 5. Principle of virtual work on a fiber strip.

Equation (11) is always true, and applies to both loading and re-loading of the flange in compression, before and after buckling. Before local buckling occurs (i.e. when the axial force N is less than critical), virtual work equation can, also, be used, but the rotation component of internal virtual work must be discarded. Buckling occurs when the external axial force reaches a critical value. After local buckling occurs, large out-of-plane deformation corresponding to the buckling amplitude results in additional internal virtual work along the yield-line plastic hinges. Therefore, the magnitude of the externally applied axial force N must decrease after buckling (after it reaches the critical buckling value) simply due to the $P-\delta$ effect at the fiber strip level. Under cyclic loading, external axial force N under such cyclic deformation is assumed to follow an elastic unloading and reloading path from and toward a yield surface, respectively.

Cross-section forces and stress distribution

Axial forces at each fiber in a cross section must be in equilibrium with externally applied moment and axial force in the plastic hinge. Axial forces in each cross-section fiber, which can be easily converted to effective stresses, are computed using either the fiber strip model describe above in the buckled region of the cross section, or the elastic-plastic stress-strain relation for the stable (un-buckled) portion of the cross section. A possible fiber force distribution in a plastic hinge section after buckling is shown in Fig. 6. In the buckled portion of section, a weak form of equilibrium of the yield-line plastic hinge was formulated to compute effective fiber force distribution (YLPH in Fig. 6). Assuming that plane sections remains plane at the boundaries of the yield line plastic hinge mechanism (Bernoulli's assumption), a simple constitutive relation for elastic-perfectly-plastic material was applied to compute the force distribution in the stable portion of section (FCS). Given a candidate force distribution it can be integrated to produce cross-section moment and axial force. These values depend on the location where web buckling initiates, defined by a distance y_m in Fig. 3. Iteration on y_m is conducted to enforce cross-section moment and axial force equilibrium.

Note that as the rotation of the plastic hinge grows, buckling amplitudes in the flange and the web grow according to the kinematics to satisfy geometric compatibility, internal work on the yield lines increases, resulting in a reduction of the average compression force in the compressed part of the cross section. This, in turn, causes a reduction in tensile force, a shift of the neutral axis, a reduction in the moment arm, and a drop in plastic hinge moment resistance.

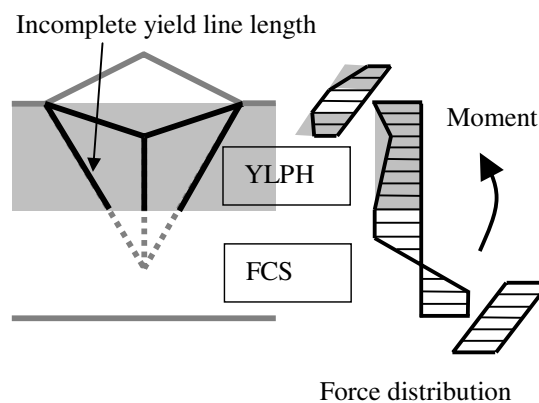


Fig. 6. Force distribution in a plastic hinge cross section.

Ultimate strain criterion

Available rotation capacity of a beam-column connection has been defined as the rotation when the strength of the connection falls below the nominal plastic strength of the beam or when it drops below 80% of the highest achieved moment resistance (FEMA-350 [1]). Cross-section equilibrium iteration, described above, can be used to establish this rotation capacity.

However, tension fracture of a flange can also be used as a criterion to determine rotation capacity. For example, cracks may form along yield lines of the buckled flanges if the monotonic tensile strain capacity ϵ_u for the material is attained during plastic hinge deformation. Note that yield line rotation may induce tension at the convex surface of the buckled flange despite the overall compression of the buckled region. Fracture strains on the yield line surface may be related to fracture rotation and resistance of the plastic hinge using the yield line plastic mechanism as follows.

Let the length of a plastic hinge along the yield lines l_{ph} be equal to plate thickness, as shown in Fig. 7. Assume curvature is uniformly distributed over l_{ph} and that the center-line of the flange plate does not deform. This assumption is consistent with the decomposition of fiber strip deformation into axial shortening of the plastic zones and rotation of the yield lines. Then, a relation between yield-line rotation and strain at the critical surface of the yield line can be expressed as [10]:

$$\begin{aligned}\Delta\theta^{YL} &= \kappa \cdot l_{ph} \\ \epsilon_f &= \kappa \cdot \frac{t_f}{2}\end{aligned}\tag{13}$$

Such plastic deformation of the yield line, with a yield-line plastic hinge length equal to flange thickness is assumed to occur only when yield-lines form, i.e. when the fiber strip buckles, and the externally applied axial force N is critical. Setting the critical strain equal to the ultimate tension strain capacity implies a corresponding critical plastic hinge rotation. Then, using kinematics, this yield line rotation can be related to the overall plastic hinge rotation to give the plastic hinge rotation capacity.

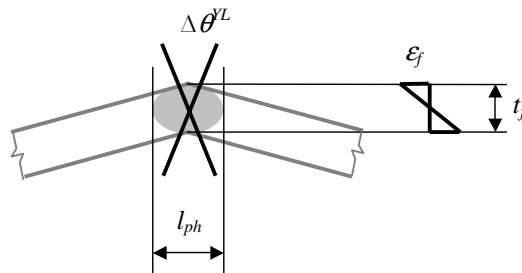


Fig. 7. Fracture on a critical yield line of plate.

SEISMIC ROTATION CAPACITY EXAMPLE

An exterior connection half-span sub-assembly was modeled to investigate connection stability. ASTM A572 Grade 50 W14×257 column and W30×99 beam are taken as the base model for this paper [11]. Normalized slenderness of the base model computed using Equation (14) and (15) is equal to one. When normalized slenderness is larger than 1.0, the cross section element is slender beyond what is permitted by AISC Seismic Provisions 2002 [12]. Normalized flange slenderness λ_f and normalized web slenderness λ_w are:

$$\lambda_f = \left[\frac{b_f}{2t_f} \right] / \left[0.30 \sqrt{\frac{E}{f_{yf}}} \right] \quad (14)$$

$$\lambda_w = \left[\frac{h}{t_w} \right] / \left[3.14 \sqrt{\frac{E}{f_{yw}}} \right] \quad (15)$$

A bilinear material model with strain hardening was used with the following properties: yield stress of 50ksi, ultimate stress of 65ksi, elastic modulus of 29000ksi, and hardening modulus of 600ksi. In this parametric study, the beam-column connection was assumed to be the WUF-W FEMA-350 connection.

The model of the exterior connection sub-assembly comprised of a rotational spring, a yield-line plastic hinge, and a fiber cross section cantilever, as shown in Fig. 8. The rotational spring represents the elastic bending behavior of the column. A yield-line plastic hinge model determines the moment and rotation of the buckled portion of the beam. Deformation of the stable portion of the beam is, finally, calculated using a curvature distribution corresponding to a linear moment distribution over the cantilever span. The curvature of the cantilever sections was computed using a fiber cross-section model in FEDEAS [13]. This was done because some of the sections may be partially yielded, but not buckled. Beam tip displacement Δ_{CL} is obtained, after applying the virtual force principle, as:

$$\delta F \cdot \Delta_{CL} = \underbrace{\delta M_{col} \cdot \theta_{col}}_{Spring} + \underbrace{\int_{buckled} \delta M \cdot \kappa dl}_{YLPH} + \underbrace{\int_{plane} \delta M \cdot \kappa dl}_{FCS} \quad (16)$$

The story drift angle was defined as the ratio of the tip displacement with respect to the un-deformed centerline of beam divided by the beam length measured from the column centerline to beam mid-span.

The model was loaded under drift control. The drift angle cyclic load history, shown in Fig. 8, followed the FEMA/SAC loading protocol defined in FEMA-350 Table 3-14. The cycles are symmetric with respect to peak drift.

Strength degradation limit state

The yield-line plastic hinge model was used to determine the load-deformation hysteretic behavior of the sub-assembly. The computed model response, in terms of normalized plastic hinge moment versus story drift, is shown in Fig. 9.

The limit states specified in FEMA-350 in terms of connection rotation drift angles are investigated next. A drift angle corresponding to the onset of local flange buckling of the beam is close to the 0.02 radian limit drift angle capacity for the Immediate Occupancy limit state. Connection resistance fell below 80% of its peak strength (approximately equal to the beam nominal strength in this example) at a drift angle of 0.03. This suggests that the rotation capacity of this connection based on the strength drop criterion is less than 0.04 radian drift value for the Collapse Prevention limit state in FEMA-350 and less than the minimum requirement of connection pre-qualification. Such result is a consequence of the conservative

assumptions adopted to formulate the YLPH model: beam moment resistance obtained using the YLPH is smaller than the actual strength, resulting in a more rapid strength degradation rate obtained from the model. Thus, a modified strength degradation rule, allowing a more severe strength drop, should be used with this yield-line plastic hinge model in order to obtain results consistent with FEMA-350.

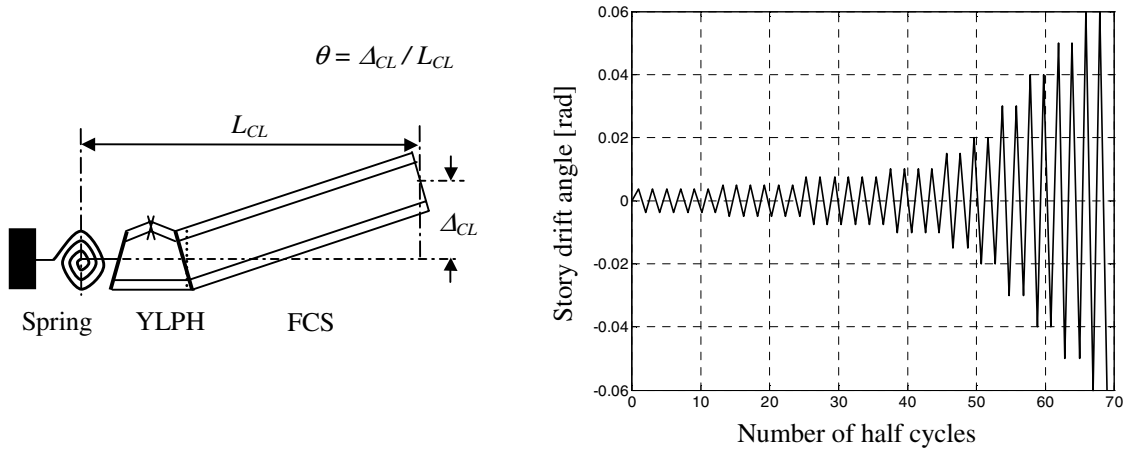


Fig. 8. Definition of model rotation and the FEMA/SAC loading protocol.

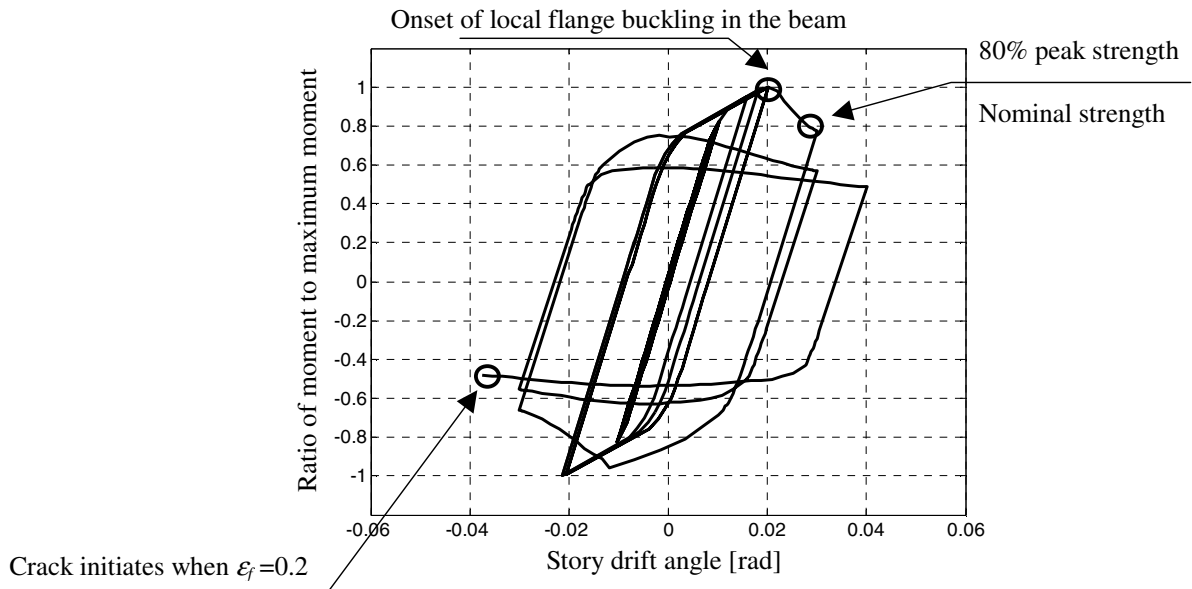


Fig. 9. Moment versus drift angle hysteretic response of the YLPH model under cyclic loading.

Low-cycle fatigue limit state

In keeping with the spirit of deformation-based design, FEMA-350 Collapse Prevention limit state may be related to initiation of flange fracture in the plastic hinge model using a low-cycle fatigue limit state. Several steps must be taken to evaluate the low-cycle fatigue limit state under the variable-amplitude FEMA/SAC loading protocol.

First, the tensile strain capacity at the critical point on a yield line of the buckled flange was assumed to be 0.2, which corresponds to the ultimate steel strain achieved in monotonic axial tension tests. This strain limit was used in the YLPH model to determine the corresponding number of cycles to failure under a constant-amplitude drift angle loading history. These analyses showed that the constant-amplitude drift angle loading history results in an incrementally increasing yield-line strain amplitude sequence because of the inability of the buckled flange to straighten and the resulting cumulative buckling deformation.

A Manson-Coffin relation between the drift angle amplitude and the number of half-cycles to failure (fatigue life) was developed by conducting a series of analyses at different constant amplitude levels, shown in Fig. 10. Both total and plastic drift angle fatigue plot are in good agreement with Manson-Coffin relations for total and plastic strain. Linear least square fitting of the YLPH model results produced material property values of $m = 2.52$ for the total drift angle and $m = 2.12$ for the plastic drift angle. These values are, also, in good agreement with values obtained by analyzing the available experimental data [14].

Fig. 10 also shows a log-log plot comparing the constant-amplitude plastic drift loading with the FEMA/SAC variable plastic drift loading in terms of the equivalent number of cycles to failure. Critical yield-line strain histories computed using the YLPH model were used to compute the equivalent number of drift cycles to failure in each case. A rain-flow cycle counting method was used first to compute the number of strain cycles at the crucial yield-line. Then, using the $S-N$ line slope $m = 2.12$ computed for plastic drift, Miner's rule was applied to get an equivalent Manson-Coffin relation, assuming that a damage index $D = 1.0$ when fracture occurs, i.e. when the tensile strain on the critical yield-line attains the value of ultimate tension strain. Finally, this Manson-Coffin relation was used to compute the equivalent number of constant amplitude cycles for the FEMA/SAC drift load history. The point shown in Fig. 10 corresponds to the FEMA/SAC load history applied until completion of the 0.04 radian total drift (or 0.03 radian plastic drift) cycles. This point lies on the $S-N$ line defined by the constant-amplitude load data, showing excellent agreement. This, in turn, means that FEMA-350 collapse prevention limit state of 0.04 radian and pre-qualification test rotation acceptance criteria may have a foundation in the low-cycle fatigue limit state defined at the material level. This result also shows that the YLPH model can be successfully used to predict low-cycle fatigue failure in steel moment connections.

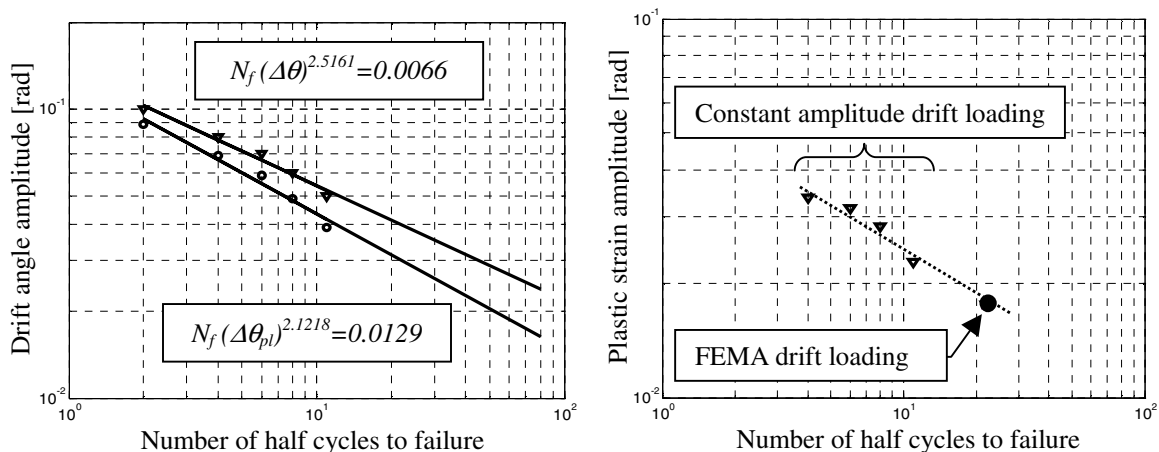


Fig. 10. Low cycle fatigue plot for drift angle and plastic strain amplitude.

CONCLUSIONS

A yield-line plastic hinge model was proposed to study local buckling behavior of US steel beam-column connections under monotonic and cyclic loading. Rotation capacity of a beam-column connection was determined with respect to strength degradation and to fracture limit states

Yield-line model approach is not commonly used to analyze steel beam-column connections. Finite element method or fracture mechanics approaches dominated the research practice in the last decade. However, the yield-line plastic hinge model approach has a distinct advantage over other approaches when post-buckling moment-rotation response of a beam-column connection is examined. Even though the yield-line approach does not yield a mechanically completely consistent solution, it offers a sufficiently accurate approximate solution. The failure criterion based on a critical yield line strain limit offers a very good estimate of plastic rotation capacity compared to a connection test results obtained during the SAC Steel Project.

A number of issues are still open. The authors are working to:

1. Improve and calibrate the model by comparing connection rotation capacities predicted by the proposed yield-line plastic hinge model to connection tests results and to finite element studies.
2. Use the yield-line plastics hinge model on different connections, such as RBS and Free Flange connections, and investigate how the model behaves under variation of beam section parameters, such as section size, and flange and web slenderness.
3. Implement the yield-line plastic hinge model in user-friendly software such that designers can use it to prototype new connections before proof-testing.

REFERENCES

1. Federal Emergency Management Agency (FEMA). "Recommended Seismic Design Criteria For New Steel Moment-Frame Buildings." FEMA Report No. 350, 2000.
2. Gioncu V, Petcu D. "Available rotation capacity of wide-flange beam and beam-columns part 1, 2." *Journal of Constructional Steel Research* 1997; 43: 161-244.
3. Anastasiadis A, Gioncu V, Mazzolani FM. "New trends in the evaluation of available ductility of steel members." *Behavior of Steel Structures in Seismic Areas STESSA 2000*; 3-26.
4. Möller M, Johansson B, Collin P. "A new analysis model of inelastic local flange buckling." *Journal of Constructional Steel Research* 1997; 43: 43-63.
5. Fisher JW, Kulak GL, Smith IFC. "A Fatigue Primer for Structural Engineering." *ATLSS Report No. 97-11*, 1997.
6. Ballio G, Castiglioni CA. "A unified approach for the design of steel structures under low and/or high cycle fatigue." *Journal of Constructional Steel Research* 1995; 34: 75-101.
7. Bernuzzi C, Calado L, Castiglioni CA. "Low-cycle fatigue of structural steel components: a method for re-analysis of test data and a design approach based on ductility." *ISET Journal of Earthquake Technology* 2000; 37(4): 47-63.
8. Collins JA. "Failure of Materials in Mechanical Design: Analysis, Prediction, Prevention." Wiley interscience publication Second Edition, 1993.
9. Lay MG. "Flange Local Buckling in Wide-Flange Shapes." *Journal of the Structural Division ASCE* 1965; ST6: 95-115.
10. Vayas I. "Investigation of the cyclic behavior of steel beams by application of low-cycle fatigue criteria." *Behavior of Steel Structures in Seismic Areas STESSA 1997*; 350-357.
11. Stojadinovic B, Goel SC, Lee KH, Margarian AG, Choi JH. "Parametric Tests on Unreinforced Steel Moment Connections." *Journal of Structural Engineering ASCE* 2000; 126(1): 40-49.

12. AISC. "Seismic Provisions for structural Steel Buildings." Chicago, IL: American Institute of Steel Construction, Inc., 2002.
13. Filippou FC. "FEDEAS: Finite Element for Design, Evaluation and Analysis of Structure." University of Berkeley, CA, 2000.
14. Lee K, Stojadinovic B. "Seismic rotation capacity and lateral bracing of US steel moment connections." Behavior of Steel Structure in Seismic Areas STESSA 2003; 335-342.